

*Article***Fluid identification method and adaptability analysis of ultra-low porosity tight sandstone in Kuqa Depression, Tarim Basin****Maojin Tan^{1,*}, Chengwen Xiao², Chuang Han², Bo Li¹, Weiping Luo², Andong Wang¹, and Qian Wang¹**

¹ School of Geophysics and Information Technology, China University of Geosciences, Beijing, 100083, China.; tanmj@cugb.edu.cn, libo@cugb.edu.cn, 2010180017@cugb.edu.cn, 2110170032@cugb.edu.cn

² Tarim Petroleum Exploration and Development Research Institute, China Petroleum, 841000, China.; xiaocw-tlm@petrochina.com.cn; hanch-tlm@petrochina.com.cn; luowp-tlm@petrochina.com.cn

* Correspondence: tanmj@cugbedu.cn; Tel.: (+86-10-82322663)

Abstract: The deep Cretaceous tight sandstone in Kuqa Depression of Tarim foreland basin is an ultra-low porosity and ultra-deep gas-bearing reservoir, which is characterized by small pores, fine throats, and poor connectivity. The wireline logging responses are so complex, and especially, it is difficult to identify fluid types from resistivity logs. Based on acoustic, density, and neutron logs response differences in gas and water layers, effective fluid sensitivity factors are constructed for gas layer identification. From conventional logs, acoustic-neutron porosity difference, density-neutron porosity difference, and triple-porosity ratio are all sensitive parameters to the gas layer. From the NMR logging response mechanism, the density and NMR porosity difference, and T2 geometric mean of the movable fluid are also two sensitive parameters to the gas layer. Based on these parameters, a series of fluid typing charts are constructed and their adaptabilities are analyzed and compared. By contrast, NMR log interpretation is better, and triple-porosity comprehensive method from conventional logs is also effective when NMR logging is not available. Finally, the comprehensive fluid typing strategy by combining some methods for ultra-low porosity tight sandstone is summarized and optimized. This study is another alternative for fluid identification using non-electrical logs.

Keywords: Ultra-low porosity tight sandstone; fluid identification; NMR logging; triple-porosity comprehensive method; integrated method

1. Introduction

The deep Cretaceous tight sandstone gas-bearing reservoir was found developed in Kuqa Depression in Tarim foreland Basin, China. The target layer is the Cretaceous Bashkirchik Formation with a burial depth of more than 6000 meters. It is an ultra-low porosity and ultra-deep sandstone reservoir, which is characterized by small pores, fine throats, and poor connectivity. Due to the high and steep structural dip and high-stress extrusion of the target reservoir, the formation is seriously heterogeneous, whose pore structure is complex, and some fractures in some intervals are developed. The minerals such as clay and chloride salts. The wireline logging responses are so complex in different types of fluids layers, and it is difficult to identify fluid types from resistivity logs because there is no difference in resistivity logs, the previous log interpretation method for natural gas reservoirs is no longer applicable [1-3].

In fluid identification of tight sandstone, a common method is to make a resistivity-porosity cross-plot. Besides, a gas-water index method and a fluid compression coefficient method were comprehensively used [4]. Li et al. also proposed index methods for identifying oil or gas layers from wireline logs of low-porosity and low-permeability sandstones in Shiwu Oilfield, China, and established a comprehensive fluid identification index [5]. Li et al. used resistivity-porosity cross-plot and lateral-induced resistivity ratio method to identify the fluid types in the Xujiahe Formation [6].

However, the porosity of tight sandstone reservoirs in Kuqa Depression is ultra-low, and the fluid in the pores is not sensitive to the logging responses. The above method is not suitable, and gas layers are difficult to distinguish from water layers from the resistivity logs [7]. Besides, new logging techniques, such as NMR logging, can improve the log interpretation accuracy of tight sandstone [8-10]. Although the investigation range of the NMR logging is in range of flushed-zone, the NMR logs contain the fluid information of mud filtrate and formation water. Huang et al. and Tan et al. used the NMR logging to evaluate the pore structure of tight sandstone reservoirs, and established a correlation between the cementation index and saturation index and T2 geometric mean [9,10]. But, in ultra-low porosity reservoirs, logs fluid typing method from NMR logging and other non-electrical need to investigate [11-12].

This work focuses on the response mechanism of acoustic, density, and neutron logs, and NMR logs, and constructed effective fluid sensitivity factors through analyzing the logs response difference between gas and water layers. Finally, a series of fluid identification methods are developed. This study is another alternative for fluid identification using non-electrical logs.

2. Geological Characteristics

The Kuqa Foreland Basin is located in the north of the Tarim Basin and south of the South Tianshan Orogenic Belt, China. It has deposited huge Mesozoic and Cenozoic strata with a thickness of more than 10km. A strong tectonic movement in the late Tertiary of the Kuqa depression formed a series of thrust nappe structures in the Kuqa depression. The fault leading to the source rocks is the main channel for oil and gas migration. Below the Tertiary gypsum mudstone and Jurassic mudstone cap is the main place for hydrocarbon accumulation.

The Lower Cretaceous in the Cretaceous in the Kuqa Depression is developed, and the Upper Cretaceous was ablated. The Lower Cretaceous is generally parallel unconformity, and the local angle unconformity on the Jurassic, with a maximum thickness of more than 3450 m. From the bottom to the top, the Cretaceous formation can be divided into the Yagliemu Formation, Shushanhe Formation, Basquique Formation, and Bashkirchik Formation. The Cretaceous Bashkirchik Formation is the main reservoir.

The Bashkirchik Formation is a set of fan delta-braided river delta sedimentary terrigenous clastic rock layers, mainly including sandstone and conglomerate, and it is characterized by ultra-low porosity and low-permeability. According to the results of rock slice analysis, the rock types of the reservoirs in the Dabei and Keshen, two main regions, are mainly lithic feldspar sandstones, most of which are less than 0.25mm in diameter, and they are mainly fine-grained sandstones and some coarse-grained sandstones. The triangle diagram of its mineral content is shown in Figure 2, and the rock lithology is mainly lithic feldspar sandstone and feldspar lithic sandstone.

Core analysis of the Bashkirchik Formation shows that its porosity and permeability characteristics, as shown in Figure 3. The porosity mainly ranges from 1.5% to 7.5%, and the permeability ranges from 0.01 mD to 0.5mD. Two porosity correlations are constructed from acoustic and density logs, and the acoustic matrix is about 53.0 us/ft, and the density matrix is about 2.68g/cm³.

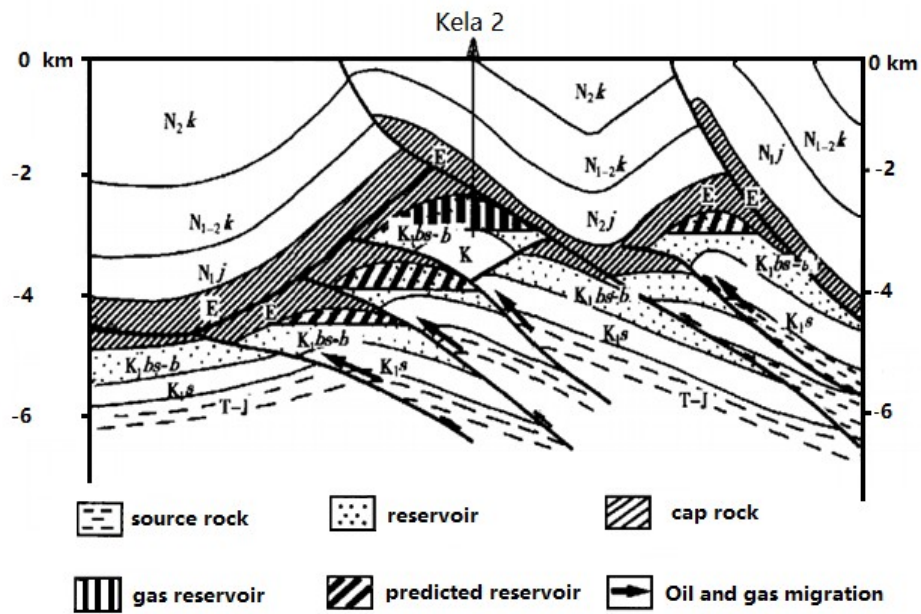


Figure 1 Hydrocarbon accumulation model of the Kelasu structural belt in the Kuqa Depression in Tarim foreland basin.

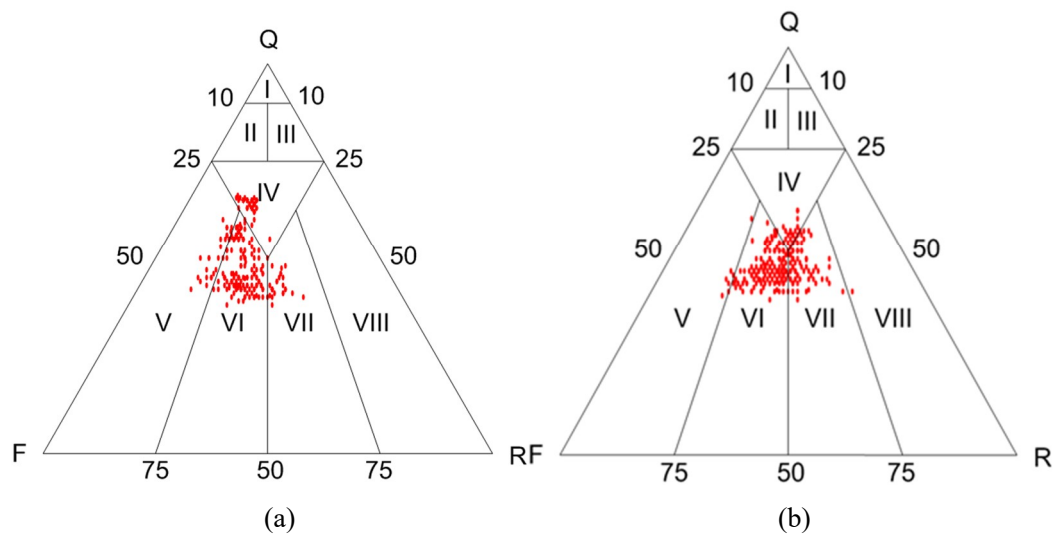


Figure 2 Lithology classification of (a) Dabei and (b) Keshen blocks, in which I- Quartz sandstone, II- Feldspar quartz sandstone, III- Lithic quartz sandstone, IV- Feldspar quartz sandstone, V- Feldspar sandstone, VI- Lithic feldspar sandstone, VII- Feldspar lithic sandstone, and VIII- Lithic sandstone.

3. Fluid identification method

3.1. Logging response of reservoirs

In the study area, Logs include natural gamma (GR), well diameter (CAL), resistivity logging (M2R1, M2R2, M2R3, M2R6, M2R9, M2RX), compensated acoustic waves (DT), compensation Neutron (CNL), compensation density (DEN), etc. Besides, NMR logging was run in individual wells.

Generally, for reservoirs saturated with oil, gas, and water, the logging responses are different from each other. Therefore, fluid identification can be performed based on the differences in logging responses. In gas layers, The conventional log responses are: (1) The resistivity of the gas layer is significantly higher than the resistivity of the surrounding bed and water layer, and the resistivity of the oil layer under the same reservoir conditions is similar or slightly higher; (2) the acoustic log shows the cycle jumping or long transit time; (3) the value of density log in the gas layer is smaller than that of the oil or water layer because the bulk density of natural gas is much smaller than that of oil or water; (4) The value of neutron log is smaller than the actual porosity because of the low hydrogen index of gas, which is named as “the digging effect”.

In high porosity reservoirs with good pore structure, the wireline log responses are different in gas layers and water layers. Especially, the resistivity log is not applicable for the fluid typing. However, for ultra-low-porosity and low-permeability reservoirs with complicated pore structure, due to a little contribution of fluids, the wireline logging response to the fluid type is not sensitive and not obvious in gas layers and water layers, the fluid identification is so difficult. Therefore, we must investigate the new log interpretation method. Considering the sensitivity of the gas to acoustic, neutron, density logging, we intend to extract formation information from these logs and construct sensitive indicating parameters. Moreover, nuclear magnetic resonance (NMR) logging is a new logging technology developed in the past 20 years. It can provide accurate porosity independent of lithology, and its T_2 distribution is not only used to characterize the pore structure but also contains rich fluid information [11-12]. NMR logging mainly detects hydrogen nuclei in the pores of the formation. The amplitude and relaxation rate of the NMR resonance relaxation signals are measured to characterize the rock pore structure and identify the fluid types [13-14].

3.2. Crossplot Methods

3.2.1. Triple-porosity logs combined method

In natural gas reservoirs, because the acoustic, density, and neutron logging responses of gas and water layers are different from each other, some parameters of porosity difference and porosity ratio were constructed to analyze their differences. The specific method is introduced as follows.

According to the well logging principle, in gas layers, the calculated acoustic porosity, ϕ_S , and density porosity, ϕ_D are both larger than actual porosity, and the measured neutron porosity, ϕ_N , is lower than actual porosity [15-16]. So, we constructed two parameters. The apparent acoustic porosity subtract the apparent neutron porosity is named as acoustic-neutron porosity difference, $\Delta\phi_{NA}$; the apparent neutron porosity subtract the apparent density porosity is recorded as, $\Delta\phi_{ND}$

$$\begin{aligned}\Delta\phi_{NA} &= \phi_N - \phi_A \\ \Delta\phi_{ND} &= \phi_N - \phi_D\end{aligned}\quad (1)$$

where ϕ_S , ϕ_D , and ϕ_N are acoustic porosity, density porosity, and neutron porosity, respectively.

In terms of geophysical logging theory, two porosities differences, $\Delta\phi_{NA}$ and $\Delta\phi_{ND}$, are close to or equal to zero in the water layer, are both less than zero in the gas layer. The higher the gas saturation, and the larger two porosities difference values. If the double porosity difference curves are displayed in the interpretation track symmetrically, the gas layer can be more clearly identified.

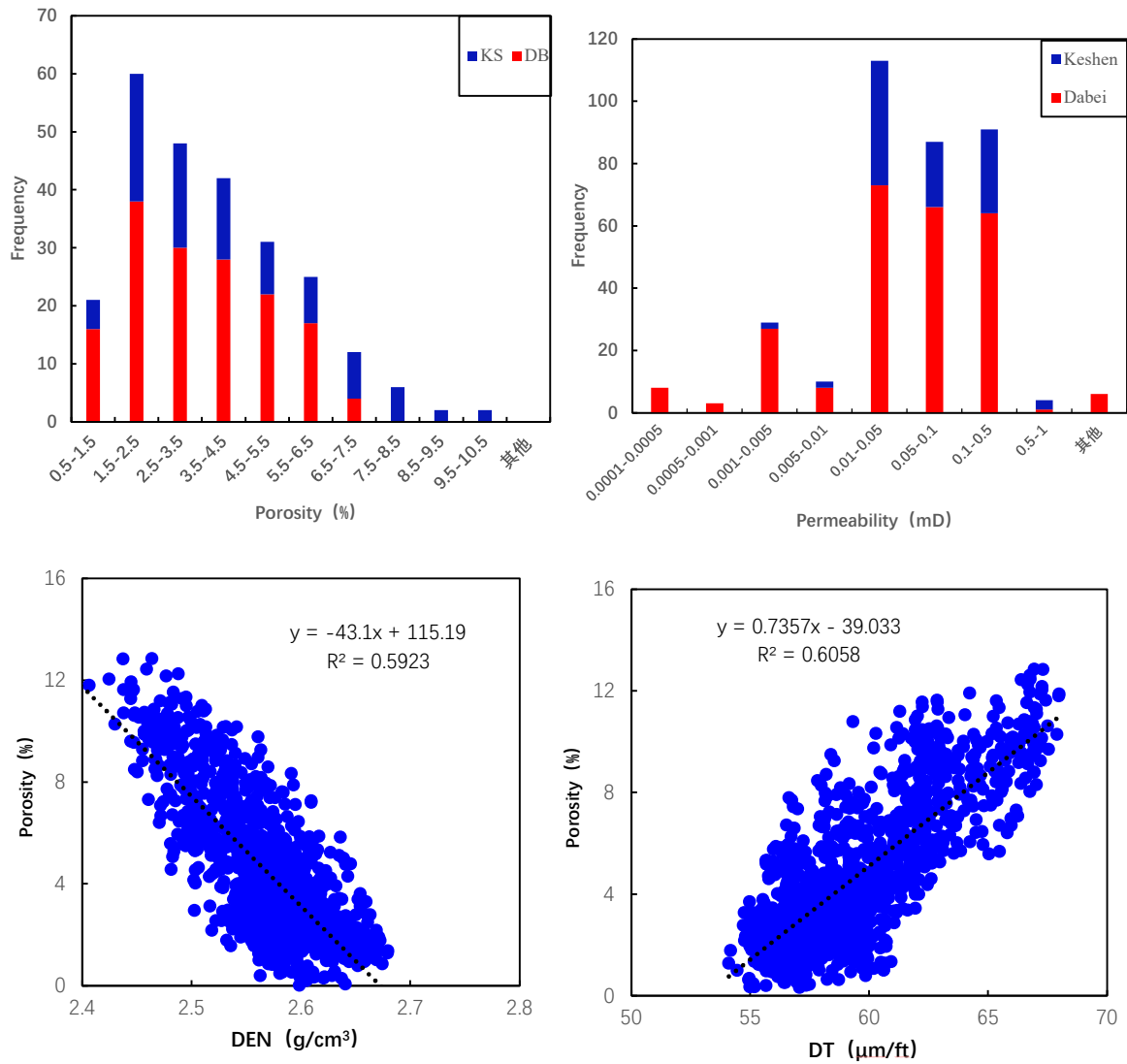


Figure 3 The porosity and permeability of Dabei and Keshen regions, and the porosity correlation with wireline logs

Besides, to further amplify the information in the reservoir, the porosity ratio is constructed, which is defined as

$$I_{SND} = \frac{\phi_S \phi_D}{\phi_N^2} \quad (7)$$

In the above formula, in water layers, I_{SND} is less than or equal to 1.0; in gas layers, because the calculated ϕ_S and ϕ_D are both overestimated, and the measured ϕ_N is underestimated, I_{SND} could be larger than 1.0.

Therefore, double-porosity differences, $\Delta\phi_{NA}$ and $\Delta\phi_{ND}$, and the ratio, I_{SND} , are parameters sensitive to the gas layer. Based on the above sensitive parameters, a series of fluid identification charts are constructed as shown in Figure 4. Four cross-plots can identify the gas layer. In Figure a, when the neutron-acoustic porosity difference is close to or less than zero, the reservoir is interpreted as a gas layer. In Figure (b), when the neutron-acoustic porosity difference is less than 0.5% and $I_{SND} > 0.8$, the reservoir is a gas layer. In Figure 6(c), when the neutron-density porosity difference is less than 0% and $I_{SND} > 0.8$, the reservoir is interpreted as a gas layer.

In Figure 4(d), when the porosity ratio is greater than 0.8 and the acoustic porosity, $\phi_S > 5.5\%$, the reservoir is interpreted as a gas layer; and the water layer can better be distinguished from the dry layer: when the porosity is less than 2%, it is interpreted as a dry layer, and when the porosity is between 2% and 5.5%, it is interpreted as water layer.

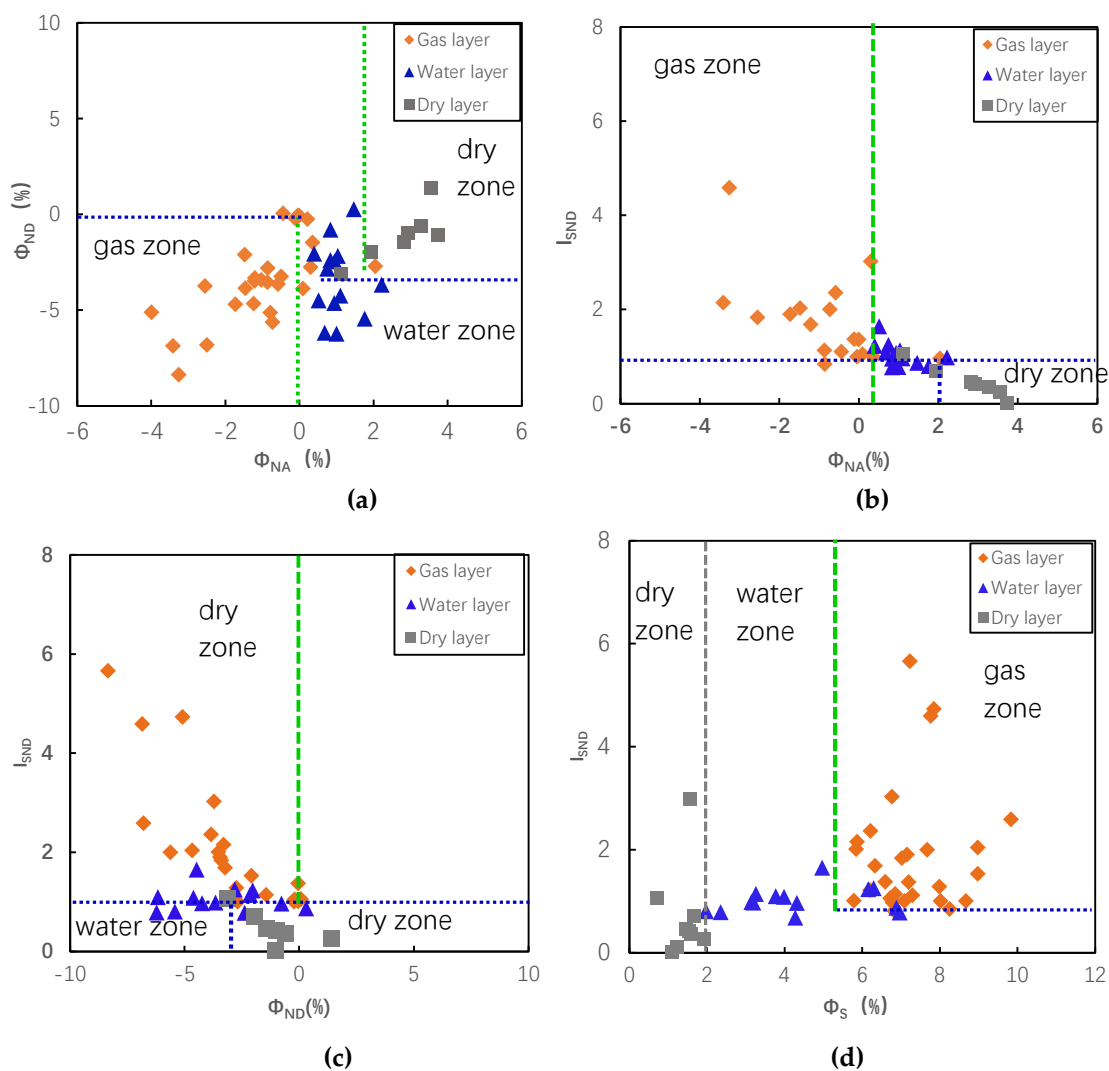


Figure 4 Two cross-plots for fluid identification including (a) $\Delta\phi_{DMR}$ -Rt cross-plot and (b) $\Delta\phi_{DMR}$ - $\Delta\phi_{MPHE}$ cross-plot

3.2.2. NMR and density logs integrated method

As well known, the depth of investigation of NMR logging is so shallow. For CMR logging technology, the depth of investigation is within 0.15 meters from the wellbore, and the flushed-zone is not the unwashed

formation [13,14,17]. For the sedimentary formation, even the lithology is complex or the reservoir is tight, the NMR technique can still accurately measure the porosity, which is one of the most important advantages of NMR logging. However, for gas-bearing or light hydrocarbon reservoirs, as the hydrogen index of natural gas is very small, the NMR log porosity is also significantly affected.

In the formation flushed-zone, the response equation of NMR logging porosity is

$$\phi_{NMR} = \phi S_{g,xo} HI_g P_g + \phi HI_f (1 - S_{g,xo}) \quad (3)$$

where ϕ is the formation porosity, HI_g is the hydrogen index, HI_f is the hydrogen index of fluid phase including the mud filtrate and formation water, $S_{g,xo}$ is the gas saturation in flushed-zone [18-20], and P_g is gas polarization function of NMR pulse sequence and the gas relaxation time. So,

$$\frac{\phi_{NMR}}{\phi} = 1 - S_{g,xo} (1 - HI_g P_g)$$

let $\alpha = 1 - HI_g P_g$, so

$$\frac{\phi_{NMR}}{\phi} = 1 - \alpha S_{g,xo} \quad (4)$$

In gas-bearing reservoirs, since $HI_g = 0.2$, $\alpha = 0.8$, the higher the gas saturation, $S_{g,xo}$, the smaller than actual porosity the NMR porosity, ϕ_{NMR} , and the lower the ratio, $\frac{\phi_{NMR}}{\phi}$. For gas layers, $\frac{\phi_{NMR}}{\phi}$ ranges from 1.1 to 1.4.

In the formation flushed-zone, the response of the density log is:

$$\rho_b = \rho_m (1 - \phi) + \rho_f \phi (1 - S_{g,xo}) + \rho_g \phi S_{g,xo}$$

where ϕ is the formation porosity, ρ_f is the density of mixed liquid phase including mud filtrate and formation water, which approximately equals 1.0g / cm³; ρ_m is the rock matrix density, according to rock physics experiments, $\rho_m = 2.68g / cm^3$.

In the log interpretation theory, the calculation method of density porosity is obtained from the density log,

$$\phi_D = \frac{\rho_m - \rho_b}{\rho_m - \rho_f} = \frac{\rho_m - [\rho_m (1 - \phi) + \rho_f \phi (1 - S_{g,xo}) + \rho_g \phi S_{g,xo}]}{\rho_m - \rho_f} \quad (5)$$

so

$$\phi_D = \phi \left[1 + S_{g,xo} \frac{\rho_f - \rho_g}{\rho_m - \rho_f} \right]$$

Let $\beta = \frac{\rho_f - \rho_g}{\rho_m - \rho_f}$, from the above formula,

$$\frac{\phi_D}{\phi} = 1 + \beta S_{g,xo} \quad (6)$$

In gas-bearing reservoirs, since $P_g = 0.2$, $\beta = 0.55$, the higher the gas saturation, $S_{g,xo}$, the larger the actual porosity the density porosity, ϕ_D , and the lower the ratio, $\frac{\phi_D}{\phi}$.

Therefore, when the formation contains gas, the NMR measurement porosity may be smaller, and the calculated density porosity is larger. To identify the types of fluid, the difference between the two porosities was selected $\Delta\phi_{DMR} = \phi_D - \phi_{NMR}$ as the sensitive indicator for fluid indication. The larger the $\Delta\phi_{DMR}$ value, the better the gas-bearing saturation of the reservoir. Therefore, the cross-plot with resistivity and NMR effective porosity (MPHE) was constructed, as shown in Figure 5. The gas layer can be successfully distinguished from the water layer and the dry layer on the cross-plot, that is, when $\Delta\phi_{DMR} \geq 3$, it is interpreted as a gas layer; when $\Delta\phi_{DMR} < 3$, it is interpreted as a water layer. Moreover, from resistivity and effective porosity, these data are overlapped together, and three fluid types are effectively distinguished from each other.

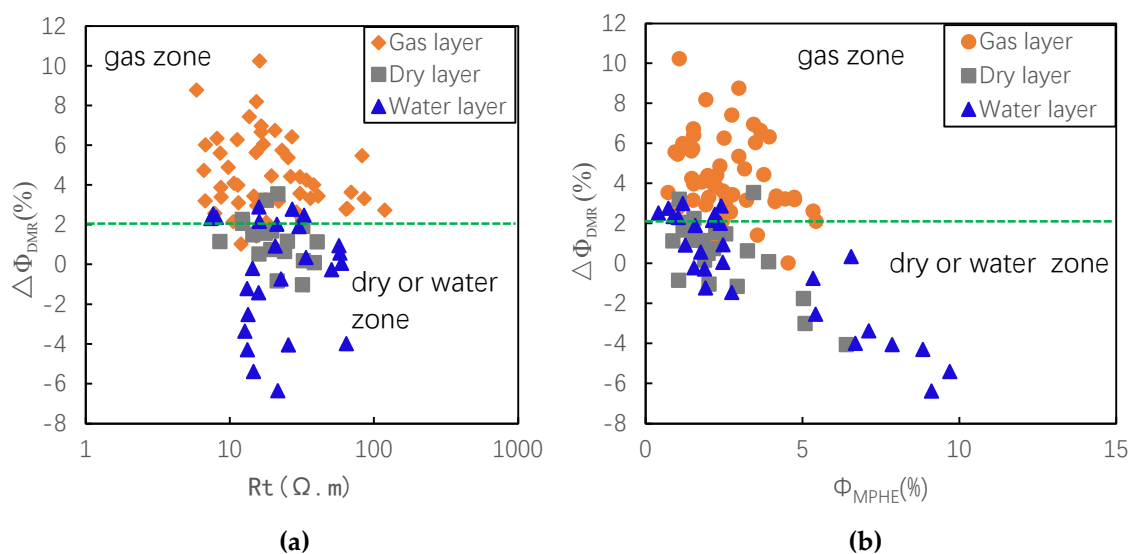


Figure 5 Some T2 geometric mean of NMR movable fluid-related cross-plots including (a) $T_{2LM} - S_{wb}$ cross-plot (b) $T_{2LM} - \Delta\phi_{DMR}$ cross-plot.

3.2.3. T2 geometric mean of NMR movable fluid-related cross-plots

According to the NMR relaxation mechanism, due to the different bulk relaxation ($T_{2\text{bulk}}$) and diffusion coefficient (D) of oil, gas, and water, the T_2 distribution of NMR log is different for rocks with the same pore structure, and its T_2 geometric mean (T_{2L}) is also different [11,16]. The bulk relaxation of natural gas is about 30-70 ms, and its diffusion coefficient is significantly larger than that of oil and water. Therefore, the T_2 geometric mean of NMR logs is a sensitive parameter to fluids and can be used for fluid identification [21-25]. Besides, because the NMR response difference between gas and water-saturated rocks is mainly in the movable fluid part of NMR T_2 distribution, the T_2 geometric mean can more clearly show the difference of different fluids. We define the T_2 geometric mean value of the NMR movable fluid part as $T_{2L,M}$, which is calculated by:

$$T_{2L,M} = \left(T_{2c}^{A_j} \cdots T_{2j}^{A_j} \cdots T_{2n}^{A_n} \right)^{\frac{1}{\sum_{j=c}^n A_j}} \quad (7)$$

where $T_{2L,M}$ is the T_2 geometric mean value of the movable fluid part; T_{2j} is the j^{th} relaxation time component, and A_j is the component porosity corresponding to T_{2j} ; T_{2c} is the bound fluid and the movable fluid T_2 cutoff value, c is the ordinal number corresponding to T_{2j} of the T_{2c} .

Two cross-plots of NMR movable fluid $T_{2L,M}$, and NMR bound water saturation (S_{wb}), $\Delta\phi_{DMR}$, are constructed as shown in Figure 6. Figure 6a is the T_{2LM} - S_{wb} cross-plot, and when $T_{2L,M}$ is between 20-125ms, the layer is interpreted as a gas layer; when $T_{2L,M}$ is less than 20ms and the irreducible water saturation is greater than 60%, the reservoir is interpreted as a dry layer. Figure 5b is the $T_{2L,M}$ - $\Delta\phi_{DMR}$ cross-plot, from which the gas layer and the water layer can be accurately distinguished. When $\Delta\phi_{DMR} \geq 3$ and $T_{2L,M}$ is between 20-125ms, the layer is interpreted as a gas layer.

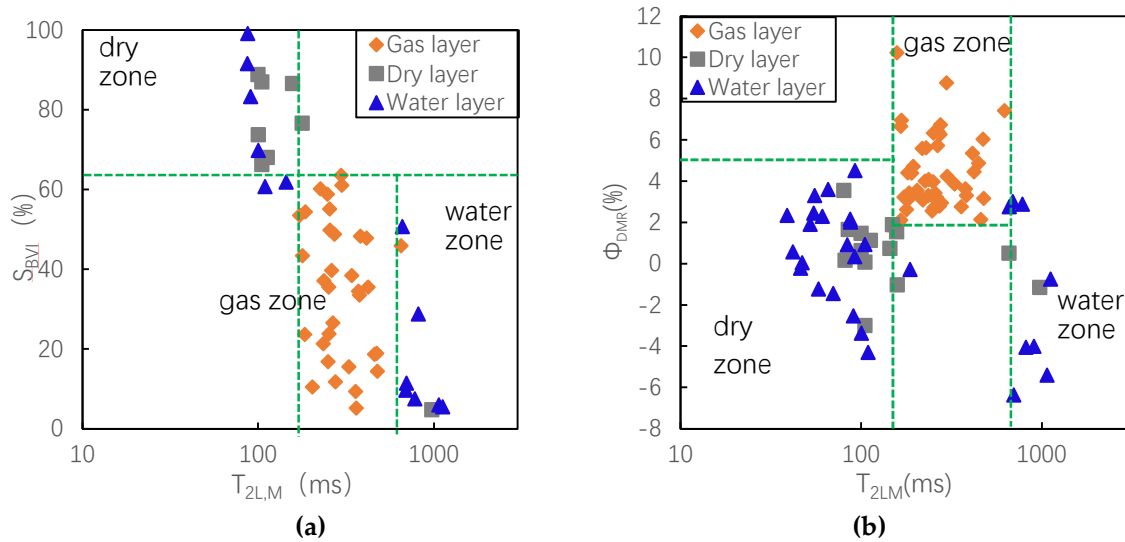


Figure 6 Triple-porosity difference and ratio method is studied and some sensitive parameters are used to construct four cross-plots for fluid typing, including (a) double-porosity difference cross-plot, (b) neutron-acoustic porosity difference and I_{SND} , (c) neutron-density porosity difference- I_{SND} cross-plot, and (d) acoustic porosity- I_{SND} cross-plot.

3.3. Adaptability Analysis of Fluid Identification Methods and Integrated Method

Among the above-mentioned fluid identification methods, their application effects are studied and compared from each other. To evaluate the effect of each method, the concept of the chart coincidence rate was proposed. The definition is the sum of the numbers of gas layers in the gas zone, the numbers of water layers in the water zone, and the numbers of dry layers in the dry zone, divided by the total number of layers. Define the chart coincidence rate (CCR) of fluid classification:

$$V_R = \frac{N_{water-layer} + N_{gas-layer} + N_{dry-layer}}{N}$$

where $N_{water-layer}$ the number of gas layers in the gas zone, $N_{gas-layer}$ is the number of water layers in the water zone, and $N_{dry-layer}$ is the number of dry layers in the dry zone. N is the sum of all layers.

Table 1 lists the fluid identification coincidence rate of different charts above.

Table 1. Fluid identification coincidence rate of different fluid identification charts

No.	Methods	Cross-plot Charts	Chart coincidence rate
1	Triple- porosity difference and ratio method	Double porosity difference cross-plot	87.96%
2		$\phi_A - I_{SND}$ cross-plot	85.67%
3		$\Delta\phi_{NA} - I_{SND}$ cross-plot	89.58%
4		$\Delta\phi_{DN} - I_{SND}$ cross-plot	85.41%
5	DMR based methods	$\Delta\phi_{DMR} - R_T$ cross-plot	84.20%
6		$\Delta\phi_{DMR} - \phi_{MPHE}$ cross-plot	84.16%
7	T_{2LM} based method	$T_{2LM} - S_{BVI}$ cross-plot	88.89%
8		$T_{2LM} - \Delta\phi_{DMR}$ cross-plot	92.90%

¹ Tables may have a footer.

In the above-mentioned NMR-related identification method, the $T_{2LM} - \Delta\phi_{DMR}$ cross-plot and $T_{2LM} - S_{wb}$ cross-plot has a higher coincidence rate and can be used to identify the gas layer. $\Delta\phi_{DMR} - R_T$ has a lower coincidence rate. The resistivity and porosity cross-plot method often used is not effective with a lower coincidence rate of about 50.6%, which shows that the resistivity is not sensitive to the gas layer. For example, in Figure 4, the resistivity of the gas, water, and dry layer overlaps together and three types are not distinguished from each other. In the triple-porosity comprehensive identification method, the $\Delta\phi_{NA} - I_{SND}$ cross-plot and the double-porosity difference cross-plot also has a higher coincidence rate, while the acoustic porosity- I_{SND} cross-plot can better distinguish the dry layer from the water layer. By contrast, the chart coincidence rate of the $T_{2LM} - \Delta\phi_{DMR}$ cross-plot is higher than that of the $\Delta\phi_{NA} - I_{SND}$ cross-plot, which indicates that NMR logging is more advantageous in gas layer identification.

Therefore, the density-NMR porosity difference, $\Delta\phi_{DMR}$, and triple-porosity ratio, I_{SND} , are two fluid-sensitive parameters. These two parameters from wireline logs amplify the effect and responses of

gas layers and make their values obvious in the gas layer. The porosity ratio in the gas layer is larger in the water layer, and it is regarded as an innovative idea for fluid identification of ultra-low porosity tight sandstone. Moreover, considering the NMR response of the gas layer, we calculated the T_2 geometric mean in the movable fluid part rather than the entire T_2 distribution, which shows more clearly the difference between the water layer and the gas layer [26].

In the logging data processing and interpretation, first, the $T_{2LM}-\Delta\phi_{DMR}$ or $\Delta\phi_{NA}-I_{SND}$ cross-plot is used to identify the gas layer, and then the acoustic porosity- I_{SND} cross-plot is used to identify the dry layer and the water layer. When NMR logging is not available, the triple-porosity comprehensive method can be used to identify gas, water, and dry layers. The Data flow for comprehensive fluid identification method is as follows:

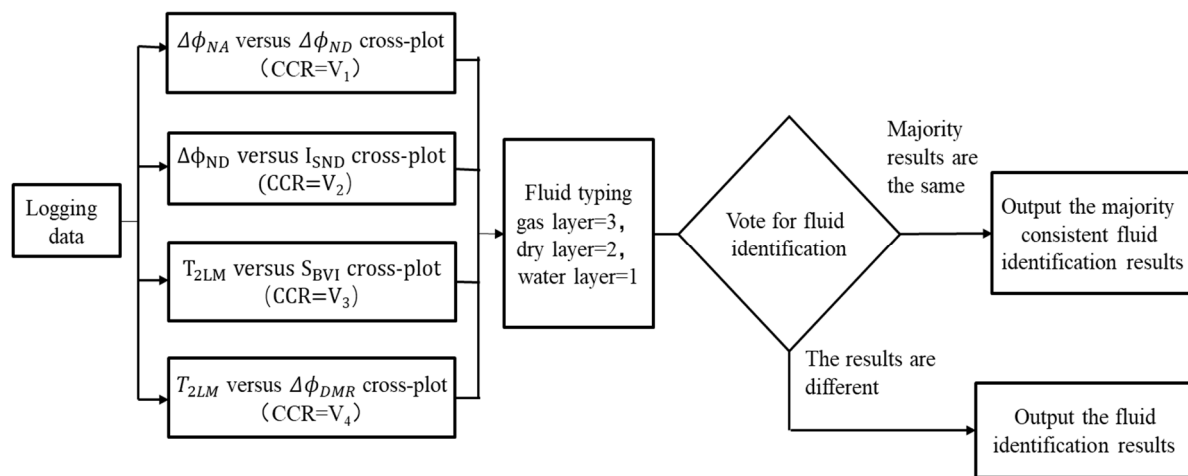


Figure 7 Data flow for the comprehensive fluid identification method

4. Case Study

Ks501 is an exploration well in the study area, and only conventionally logs are run. Because the resistivity-porosity cross-plot method cannot be used effectively for fluid typing, the density porosity, acoustic porosity difference, neutron-density porosity difference, and triple-porosity ratio, are calculated using Eq. (1) and (2). These results are shown in Figure 8. Track 3 is a resistivity log, Track shows triple-porosity log, and Track 5 shows calculated acoustic porosity, neutron acoustic porosity difference, neutron-density porosity difference, and three-porosity ratio. Comprehensive fluid identification was carried out using the differential ratio fluid identification chart. At zone of 6404-6430m, the natural gamma-ray log reads about 49.72 API, the calculated acoustic porosity is about 6.45%, the neutron-acoustic porosity difference is about -0.137%, the neutron-density porosity difference is about -1.462%, and the triple-porosity ratio is about 1.059. According to the $\Delta\phi_{NA}-I_{SND}$ cross-plot in Figure 6, it is interpreted as a gas layer, and the other three cross-plots are also interpreted as the gas layer. The product testing data shows that the gas production was 161,448 m³/day, and regards it as a gas layer, so the logs interpretation result from the triple-porosity comprehensive method is correct.

Ks204 is another exploration well in the study area. In addition to conventional logs, NMR logging was run by the CMR-plus tool, and the logging data processing was performed using the above methods. First, the neutron-acoustic porosity difference, neutron-density porosity difference, and triple-porosity ratio, I_{SND} are calculated using Eq. (1) and (2). Then, similarly, using Eq. (4) and (6), the density-NMR porosity difference,

$\Delta\phi_{DMR}$ can be calculated. The T_2 threshold cutoff value is determined from the NMR experiment of cores, and The $T_{2cutoff}$ is 16 ms through a comparison of the measurement of water saturation and after centrifugation. From Eq. (7), the T_2 geometric mean (T_{2LM}) of the movable fluid part in T_2 distribution can be calculated.

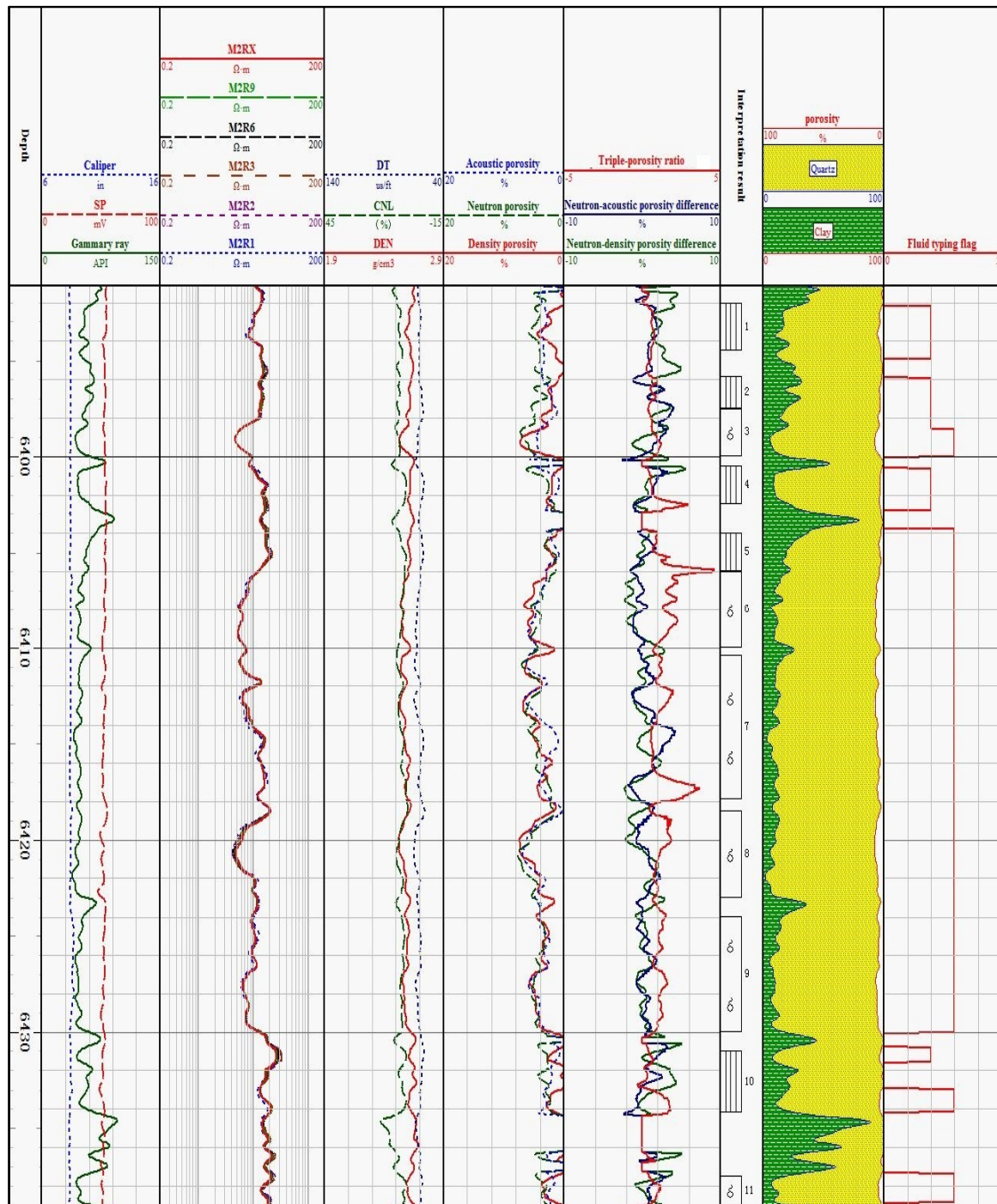


Figure 8 Logging data processing and interpretation results of Ks501

Figure 9 shows the results of logging data processing and interpretation of well Ks204. Track 3 shows the resistivity log, Track 4 shows the NMR T_2 distribution and the T_2 geometric mean of the movable fluid, Track 5 shows the density-NMR porosity difference, and Track 6 is the calculated acoustic porosity and triple-porosity ratio. The $\Delta\phi_{DMR-T_{2LM}}$ cross-plot and the triple-porosity ratio methods are integrated for log interpretation, as shown in Track 7.

At the zone of 5973 -- 5981 meters, the natural gamma-ray is low, and the NMR porosity and density porosity are about 4% and 10%, respectively. The calculated T_2 geometric mean of the movable fluid is about 300ms, so it is interpreted as a gas layer from the $\Delta\phi_{DMR}-T_{2LM}$ cross-plot. Moreover, the calculated acoustic porosity is about 10%, and the triple-porosity ratio, I_{SND} , is about 4%, so it is interpreted as a gas layer from $\Delta\phi_{DMR}-I_{SND}$ cross-plot. Therefore, this layer in the zone of 5973 -- 5981 meters is comprehensively judged as the gas layer. The product testing data shows that the gas production was 57.38 m³/day, and the testing result indicates that it a gas layer. At the zone of 5994 -- 6000 meters, the natural gamma-ray is low, and the NMR porosity and density porosity are about 8% and 7%, respectively. The calculated T_2 geometric mean of the movable fluid is about 100ms, so it is interpreted as a water layer from the $\Delta\phi_{DMR}-T_{2LM}$ cross-plot. Therefore, this layer in the zone of 5994 -- 6000 meters is comprehensively interpreted as a water layer. The product testing data shows that the water production was 18.6 m³/day, and the testing result regards it as a water layer, so the interpretation of the logs is proved correct.

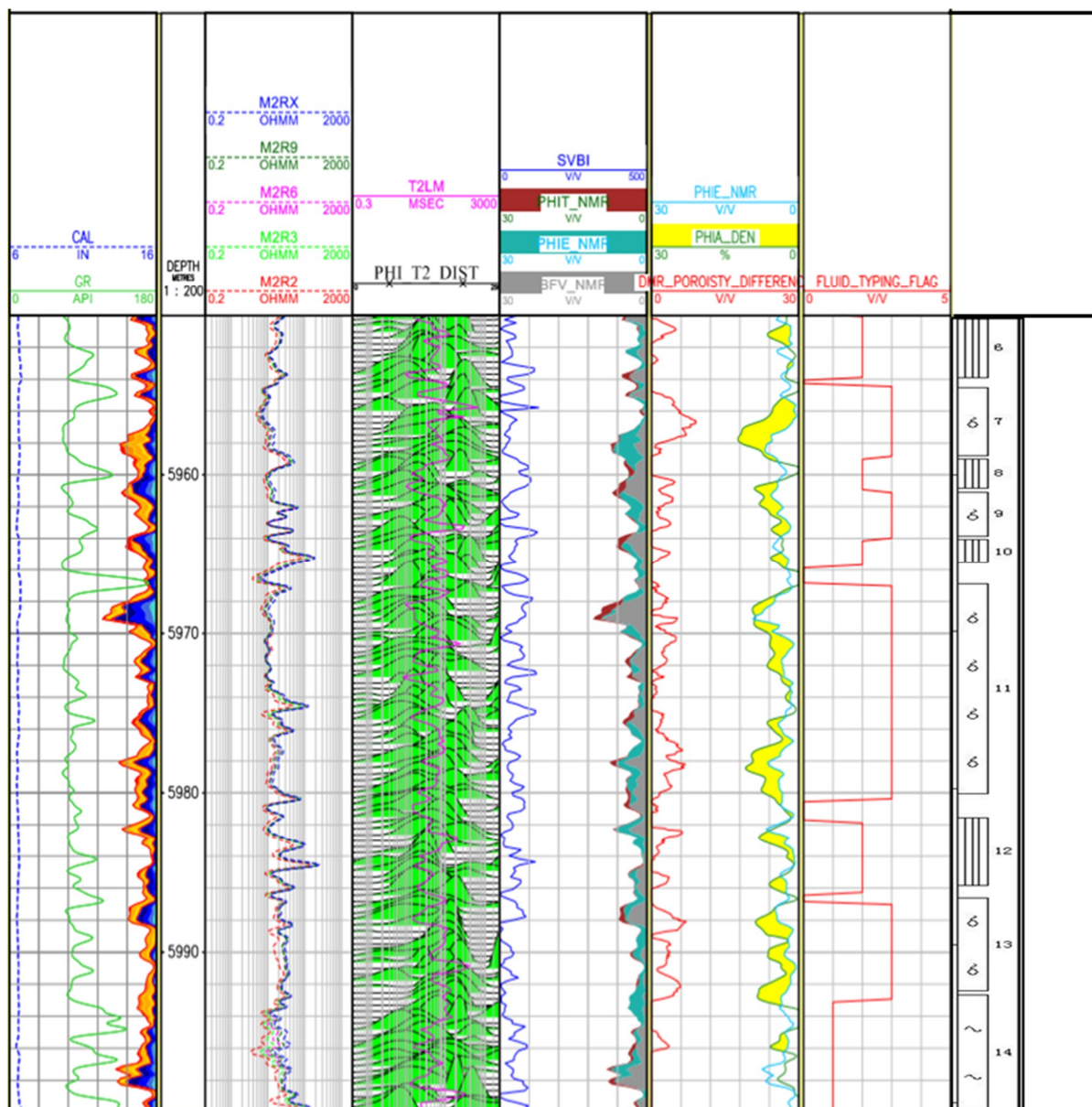


Figure 9 NMR logging data processing and interpretation results of Well Db204

Besides, NMR logging data of 8 wells were processed by using the above method and 16 layers were interpreted by the proposed method. Compared with the product test, the interpretation coincidence

rate was about 90.2%. Also, another 16 wells, whose NMR logs were not available, triple-porosity comprehensive method is used to log interpretation, 33 layers are classified and the interpretation coincidence rate was about 87.32%. The application in this study area shows that the $T_{2LM}-\Delta\phi_{DMR}$ cross-plot and triple-porosity method for fluid identification is effective in tight sandstone reservoirs in Kuqa Depression.

5. Conclusions

(1) Nuclear magnetic resonance logging can be used for fluid identification of Ultra-low porosity tight sandstone reservoirs. The density and NMR difference and T_2 geometric mean of the mobile fluid are two sensitive parameters to the gas layer. The constructed $T_{2LM}-\Delta\phi_{DMR}$ cross-plot is effectively applied to fluid identification in tight sandstone reservoirs.

(2) When the NMR log is not available, in conventional logs, acoustic-neutron porosity difference, density-neutron porosity difference, and triple-porosity ratio are all sensitive parameters to the gas layer. Four fluid identification charts based on the porosity difference and ratio can also achieve fluid identification.

(3) The $T_{2LM}-\Delta\phi_{DMR}$ cross-plot method from NMR logging is better than the porosity ratio method from conventional logs, which indicates the advantages of NMR logging.

Author Contributions: Conceptualization, M.T. and CW.X.; methodology, M.T. and CW.X.; software, B.L.; validation, C.H., CW.X. and WP.L.; formal analysis, AD.W.; investigation, M.T.; resources, C.H.; data curation, AD.W.; writing—original draft preparation, M.T.; writing—review and editing, M.T.; visualization, Q.W.; supervision, M.T.; project administration, CW.X.; funding acquisition, CW.X. All authors have read and agreed to the published version of the manuscript.

Funding: This research was funded by the National Natural Science Foundation of China, grant number 41774144, U1403191”.

Acknowledgments: This work presented is sponsored by National Major Projects "Development of Major Oil& Gas Fields and Coal Bed Methane" (2016ZX05014-001), and the Fundamental Research Funds for the Central Universities (292015209).

Conflicts of Interest: The authors declare no conflict of interest. The funders had no role in the design of the study; in the collection, analyses, or interpretation of data; in the writing of the manuscript, or in the decision to publish the results.

Corresponding Author: Maojin Tan is a professor at the China University of Geosciences (Beijing). He obtained his Ph.D. in 2006, and worked as a postdoctoral fellow in Geophysics from 2006 to 2008, at the Graduate University of Chinese Academy of Sciences. His research interests focus on geophysical well logging with emphasis on new logging technologies and formation evaluation of complex reservoirs. So far, he has published 42 papers in technical journals such as "Geophysics", "Journal of Applied Geophysics", and "Computer and Geosciences".

References

1. Michael, E.M., Dale, F., Tom, R., 2008. Tight gas surveillance and characterization: impact of production logging. *SPE Unconventional Reservoirs Conference*, 2008(2), Keystone, Colorado.
2. Yang, H.J.; Zhang, R.H.; Yang X.Z. Characteristics and reservoir improvement effect of structural fracture in ultra-deep times sandstone reservoir: Cases study of Keshen, Gasfield, Kuqa, Depression, Tarim, Basin. *Natural Gas, Geoscience*, **2018**, 29 (7): 942-950
3. Xin, Y.; Tang, J.; Luo, Z.Y.; Bie, K.; Tang, B.Y., Li X.L. Logging Evaluation for Sandstone Reservoirs in Bashijiqike Formation of Keshen Area, Kuqa Depression. *Xinjiang Petroleum Geology*, **2019**, 40(1): 116-121
4. Zhang, S.N., 2008. Tight sandstone gas reservoir: their origin and discussion. *Oil & Gas Geology*, **2008**, 29(1):1-10.

5. Li, W.; Yang X.; Cao, Y. Logging identification technology for low permeability reservoir in Shiwu oilfield. *Journal of Jilin University (Earth Science Edition)*, **2010**, S1: 94-101.
6. Li M., Lai Q., Huang K. Logging identification of fluid properties in low porosity and low permeability clastic reservoir: A case study of Xujiahe gas reservoir in the Anyue gas field, Sichuan basin. *Natural Gas Industry*, **2013**, 33(6): 34-38.
7. Li, N.; He X.; Gao X.L. Review and prospect of well logging evaluation technology for low porosity and low permeability reservoir. *World Well Logging Technology*, **2013**, 3: 8-11.
8. Fu, J.H.; Shi Y.J. Fine evaluation of low-permeability sandstone gas reservoir by use of nuclear magnetic resonance logging. *Nature Gas Industry*, **2002**, 22(6): 39-42.
9. Huang Y.; Zhao J.; Cheng, P. Enhancing accuracy of saturation model of low-porosity and low-permeability reservoir by using nuclear magnetic resonance logging data. *Oil & Gas Geology*, **2007**, 28(3):390-394.
10. Tan, M.J., Zou, Y.L., 2010. The optimization of Archie saturation model based on NMR. *Proceedings of the 26th Annual Meeting of China Geophysical Society*, **2010**, 37-40.
11. Xiao, L.Z. Nuclear magnetic resonance (NMR) imaging logging and rock NMR and application. *Beijing: Science Press*,**1998**.
12. Coates, G.R., Xiao, L.Z. and Manfred, G.P. NMR logging principles and applications. *Houston (Texas): Sea Gulf Press*, **1999**.
13. Hou B. L., and Coates, G.R. Nuclear magnetic resonance logging methods for fluid typing, *SPE paper 48896, SPE International Conference and exhibition*, Beijing, China, 2-5 November, **1998**.
14. Minh, Ch.C.; Fredman R.; Cray, S. and Cannon, D. Integration of NMR with other openhole logs for improved evaluation, SPE paper 49012, *SPE Annual Technical Conference and Exhibition*, New Orleans, Louisiana, 27-30 September, **1998**.
15. Chu Z.H., Gao J., Huang L. Geophysical logging method and principle. *Beijing: Petroleum Industry Press*,**2008**.
16. Darwin, V.E. and Julian, M.S. Well Logging for Earth Scientists (2nd Edition), *Springer Press*, **2000**.
17. Dunn, K.J., Bergman, J. and La Torraca, G.A. Nuclear Magnetic Resonance. Petrophysical and Logging Applications, *Pergamon, an Imprint of Elsevier Science*, **2002**.
18. Abu-Shanab, M.A; Hamada G.M.; Oraby M E. DMR technique improves tight gas sand porosity estimate. *Oil & Gas- Journal*, **2005**, 103 (47): 54 - 59
19. Abu-Shanab M.M, Hamada G.M, Oraby M E, and Abdelwally A.A. Improved porosity estimation in tight gas reservoirs from NMR and density logs. *Emirates Journal for Engineering Research*, **2005**, 10 (2): 9-13
20. Prammer, M.G.; Mardon, D. Lithology-Independent Gas Detection by Gradient NMR Logging, *SPE30562*, **1995**.
21. Agut, R., Levallois, B. and Klopff, W. Integrating core measurements and NMR logs in complex lithology, *SPE paper 63211, SPE Annual Technical Conference and Exhibition, Dallas Texas*, **2000**, 1-4 October.
22. Freedman, R. Advances in NMR logging, *JPT-January*, **2006**, pp.60-66.
23. Xiao, L.Z.; Xie, R.R.; and Liao, G.Z. NMR logging theory and method of China complex reservoirs. Beijing: Science Press (in Chinese), **2012**.
24. Hamada, G.M.; Oraby, M.E. Integration of NMR with other open hole logs for improved porosity, permeability and capillary pressure of gas sand reservoirs. *SPE 119064*, **2007**.
25. Hamada, G.M.; AbuShanab, M A. Better porosity estimate of gas sandstone reservoir using density and NMR logging data. *SPE 106627*, **2007**
26. Hamada, G.M.; AbuShanab, M.A. Petrophysical properties evaluation of tight gas sand reservoir using NMR and conventional openhole logs. *SPE 114254*, **2008**